

EXPERIMENTAL QUANTIFICATION OF ULTRAVIOLET RADIATIONS AND BIOCIDAL ACTIVE SPECIES IN MICROWAVE ARGON PLASMA JET IN OPEN AIR

G. WATTIEAUX^{1*}, F. JUDÉE¹, N. MERBAHI¹, M. YOUSFI¹, M.P. CASTANIÉ-CORNET²,
M. MANSOUR²

¹ LAPLACE / UMR 5213

² LMGM / UMR 5100

CNRS, Université de Toulouse, 118, route de Narbonne 31062 Toulouse Cedex 9 France

*wattieux@laplace.univ-tlse.fr

ABSTRACT

Absorption and mainly emission spectrometry have been used to identify active species generated by a microwave induced surfatron plasma jet launched in open air and using argon flowing gas. The argon flow rate is kept constant at 1 L/min and the microwave power is 40 W. We determined the ozone and atomic oxygen concentrations, ultraviolet C (UVC) irradiance, gas temperature, plasma electron density and excitation temperature. Most of these diagnostics are spatially resolved along the plasma jet axis. Assessment of the biocidal efficiency of the present low temperature plasma will be shown in the case of standard Gram-negative bacteria (*Escherichia coli*) and the main germicidal source of the jet is identified. A specific emphasis has been done for human health hazard assessment since simple solutions are reminded to respect safety standards for exposures to ozone and microwave leakage. These solutions should be adopted by users of microwave induced plasma in open air conditions because, according to the literature, this is not often the case.

1. EXPERIMENTAL SETUP

The present study is performed by using a standard surfatron [1] generating surface microwaves able to ignite a gas discharge inside a quartz tube placed inside the center of the setup as displayed in the scheme of figure 1. The quartz tube having 4 mm and 6 mm for the inner and outer diameters is surrounded by the surfatron cavity with a 2 cm length extending in the downstream side out this cavity. A Sairem solid state microwave generator

operating at a frequency of 2.45 GHz in continuous mode is connected to the applicator of the surfatron. The microwave output power is 40 W.

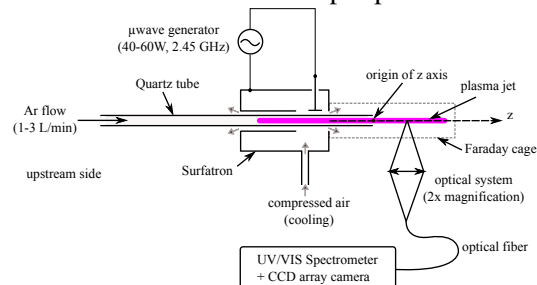


Fig. 1: Schematic view of the experimental setup with the microwave source, the gas flow inlet, the gas cooling, the spectroscopy device, the Faraday cage and the plasma jet launched in the downstream side along the z axis having its origin at the glass tube outlet.



Fig. 2: Fast imaging of the plasma jet at the tube outlet with an ICCD camera. Time of exposure: $1\mu\text{s}$

The argon working gas (with purity grade of 4.5) is injected in the quartz tube through a mass flow controller placed in the upstream side. In this study the argon flow rate is kept constant at 1 liter per minute (L/min). Due to the presence of surface microwaves the plasma does not fill the whole cross section of the quartz tube. When launched in ambient air, the plasma covers preferentially the external zones prolonging the tube edges. Following the recommendation of the manufacturer, the quartz tube is cooled by compressed air escaping from the surfatron body by flowing along the tube in the upstream direction and in the downstream direction. Therefore compressed air cools down the plasma jet while mixes with it due to air tur-

bulences at the edge of the tube outlet. In this case, random occurrence of filamentary structures are observed at the tube outlet (see fig. 2). This arrangement enables to keep the gas temperature below 325 K in the vicinity of the quartz tube outlet in the operating conditions of this study. The surfatron microwave leakage has been estimated when the discharge is ignited by multiplying the microwave irradiance value measured with a Sairem IFP 05 C microwave irradiance meter set 10 cm away from the surfatron body by the surface of a 10 cm radius sphere. According to this procedure, the microwave leakage represents about 5% of the power delivered by the generator whatever the input microwave power and argon flow levels. These measurements have been performed without the Faraday cage (displayed in fig. 1). It has been found that the microwave leakage does not meet safety requirements ($5\text{mW}/\text{cm}^2$ at 5 cm away from the source) as soon as the input power exceeds 30 W. This is why a Faraday cage is set in the downstream side in order to cover the tube part outside the surfatron setup (see fig. 1).

Lateral radiations of the plasma jet are collected by a 2x magnification optical system offering a 1 mm spatial resolution. It is mounted on a sliding stand to perform a scan along the plasma jet axis (see fig. 1). The plasma radiations are guided through an optical fiber (UV-silicon LG-455-020-3) onto the entrance slit (100 μm wide) of a 0.5 m imaging spectrophotometer (Acton Spectra Pro 2500i, in the Czerny–Turner configuration). The detecting device is a CCD camera (PIXIS -256E, 256×1024 imaging array of $26 \mu\text{m} \times 26 \mu\text{m}$ pixels) which is placed at its exit port. Its spectral domain lies within 200 nm and 920 nm. Analysis are performed using a 2400 grooves/mm grating in the UV range and using a 1800 grooves/mm grating in the visible range. The spectral region which can be measured simultaneously with the CCD is about 20 nm for both gratings in their respective spectral range. An optical high pass filter is used for the visible range analysis in order to prevent any perturbation of the visible range spectra due to the unwanted grating second order of diffraction of the UV light.

Finally, in order to evacuate hazardous species produced by the device such as ozone, the plasma device is set in front of an air extractor.

2. DIAGNOSTIC TOOLS

Gas temperature is estimated from the OH(A-X) molecular radiations between 306 and 310 nm by adjusting a temperature dependent synthetic spectrum on the experimental spectrum.

Electron density is deduced from the Stark broadening full width at high maximum (FWHM) w_s (see eq. 1) of the H_β line (486 nm) which is estimated after Van der Wals, Doppler and instrumental broadenings being subtracted from the experimental broadening of the line [1].

$$w_s (nm) \approx 4.8 \times \left(\frac{n_e (m^{-3})}{10^{23}} \right)^{0.68} \quad (1)$$

The excitation temperature T_{exc} of argon neutral atoms was determined from a Boltzmann plot assuming a Boltzmann distribution of the different ArI excited levels E_i in the flame (4p, 5p and above)

The ozone number concentration $[O_3]$ is determined from the absorption of the mercury line at 253.7 nm. The concentration of this molecule is probed 30 mm after the tube outlet in the axis of the jet. This measurement is difficult to perform since the absorption of the mercury line by ozone molecules is very weak in our conditions (few percents).

The order of magnitude of the ground state atomic oxygen concentration is estimated from the ratio between the intensity of the O line at 844 nm and the Ar line at 852 nm. This simple method also provides the spatial distribution of the air proportion into the plasma jet [1].

Perpendicular UVC (190-280 nm) irradiance (relatively to the axis of the jet) is determined by using a photodiode which is only sensitive to radiations between 225 and 280 nm (SG01S-C18, sglux GmbH). The photocurrent is determined by short circuiting the photodiode with a transimpedance amplifier circuit having a conversion factor of 1.82 V/nA. The active area of the photodiode is 0.06 mm^2 and its quantum efficiency is about 0.1 A/W at 265 nm.

3. PLASMA DIAGNOSTICS

In our experimental conditions, the H_β line emerges from the noise from the inside of the tube up to 14 mm after the tube outlet. The FWHM of this line which corresponds to an electron density n_e of $1.2 \times 10^{14} \text{ cm}^{-3}$ does not change significantly over this span.

The rotational temperature T_{rot} of OH molecules remains rather constant at 800 K within the experimental uncertainty. Monitored up to 30 mm away from the outlet of the quartz tube by a thermocouple, the apparent temperature of the plasma jet is kept below 50°C for every experimental condition of this work by the presence of the cooling compressed air of the tube which dilutes the hot plasma jet. However the gas temperature emerging from the tube is estimated between 600°C and 800°C with a thermocouple while cooling compressed air is turned off. Motret *et al.* [2] noticed that the OH rotational temperature is strongly correlated with the gas temperature in the streamer region of a non-thermal atmospheric plasma obtained by a dielectric barrier discharge. Consequently, we concluded that the OH rotational temperature corresponds to the temperature of the plasma emerging from the tube.

All the gaseous species and especially O, NO, NH, N_2 , N_2^+ and H which are detected by emission spectroscopy into the plasma jet launched in the ambient air are also detected inside the quartz tube immediately after the surfatron exit with a quasi constant level that is comparable at the tube outlet. In the ambient air, the intensity of their respective radiations decreases along the plasma plume and vanishes at a distance of 20 mm to more than 36 mm depending on the species. Moreover, we can notice that the absolute atomic oxygen concentration [O] corresponds the level of impurity of the Ar bottle (see fig. 3.b). These findings underline that a significant part of the active species produced by the plasma jet come from the gas impurities.

Since the excitation temperature of Ar remains constant along the plasma jet ($T_{exc} \approx 4200 \text{ K}$), the spatial decay of the intensity of the Ar lines is attributed to the dilution of the Ar flow in the ambient air. Considering that the jet is only composed of Ar at the tube outlet, it is possible to

follow the spatial distribution of Ar and air into the plasma jet. The dilution of the Ar flow is displayed in figure 3.a.

The ozone concentration determined 30 mm after the tube outlet reaches $88 \pm 30 \text{ ppm}$ only 2 min after the plasma ignition with the air extractor turned off. This high level justifies the presence of an extractor next to atmospheric surfatron Ar plasma jets. This is especially required for experiments with higher microwave power.

As it can be seen in figure 4, excited NO molecules of the jet provide UVC radiation. The UVC irradiance decreases linearly with the distance from the surfatron tube outlet and the absolute level is rather important : 5 mm after the tube outlet, it reaches $65 \mu\text{W} \cdot \text{cm}^{-2}$.

Table 1 summarizes the main parameters of the plasma jet.

	$z=5\text{mm}$	$z=30\text{mm}$
n_e	$1.2 \times 10^{14} \text{ cm}^{-3}$	n/a
T_{rot}	$800 \pm 100 \text{ K}$	n/a
T_{exc}	$4200 \pm 200 \text{ K}$	$4200 \pm 200 \text{ K}$
[O ₃]	n/a	$88 \pm 30 \text{ ppm}$
[O]	80 ppm	< 10 ppm
[Ar]	100%	< 10%
UVC	$65 \mu\text{W} \cdot \text{cm}^{-2}$	$40 \mu\text{W} \cdot \text{cm}^{-2}$

Tab. 1: Parameters of the plasma jet. z is the distance from the tube outlet. n/a = not available

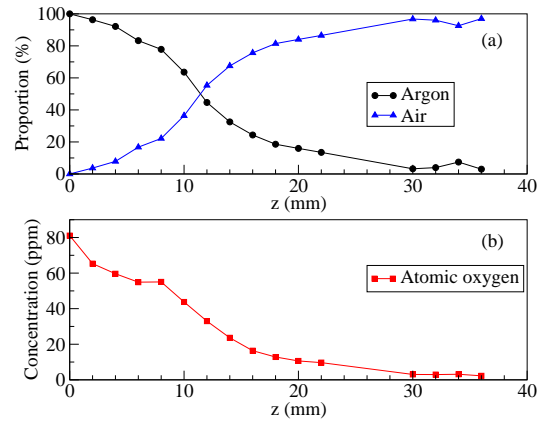


Fig. 3: Spatial evolution of Ar and air (a) and of atomic oxygen (b) concentrations in the axis of the plasma jet

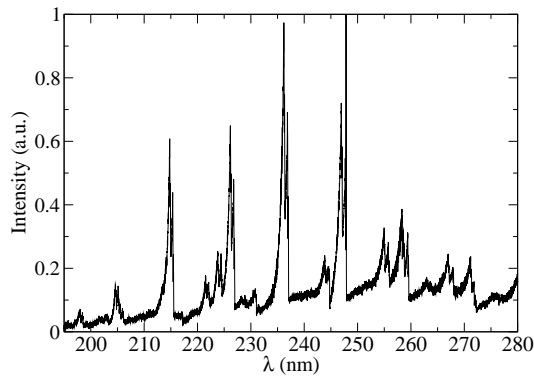


Fig. 4: Electromagnetic spectrum of the plasma jet in the UVC region. The continuum is attributed to NO_β molecules and the quasi periodic structures come from NO_γ molecules. Measurement taken in front of the jet.

4. UVC PROPORTION IN THE GERMICIDAL EFFICIENCY OF THE JET

UVC radiations are very efficient to eradicate micro organisms by altering their DNA [3]. In order to evaluate the proportion of the UVC radiations in the germicidal efficiency of the jet, two experiments have been carried out on *Escherichia coli* cells in stationary growth phase and dispersed in milliQ water.

In a first time, the biological mixture was exposed to the plasma jet during 300 s at a distance of 5 mm from the tube outlet of the surfatron. After dilution and spread on petri dish with nutrient LB medium, surviving bacteria are counted after a 15h incubation at 37°C. In the meantime, the same operation is carried out for a control mixture which has not been exposed to the plasma jet. In order to provide good statistics, this protocol is carried out 20 times. In these conditions, $97.66 \pm 1.33\%$ of the plasma exposed bacteria are killed by the plasma jet.

In a second time, a fused silica plate (optical transmission : 190-2000 nm) is placed on top of the well containing the water/bacteria mixture before plasma exposure. In this configuration $84.57 \pm 1.92\%$ of the bacteria die after plasma exposure (8 experiments). Due to the presence of the transparent plate, atomic and molecular species of the plasma jet do not reach the mixture thus the bactericide effect of the jet can only be attributed to electromagnetic radiations. As DNA absorbs radiations in the UVC region only [4], we conclude that the main bactericide effect of the plasma jet comes from UVC radiations. In order to confirm

this conclusion, we can underline that the level of exposure to UVC radiations (20 mJ) of the bacteria during our study is in accordance with the 1 log reduction of the *E. coli* population by UVC radiations previously reported [4].

5. CONCLUSION

An atmospheric Ar microwave surfatron plasma jet has been characterized and its radiations in the UVC region of the electromagnetic spectrum have been identified as the main bactericide source. These radiations come from excited NO molecules which are formed from the impurities of the argon working gas bottle. The contribution of the UVC radiations produced by the plasma jet represents $86.7 \pm 3.2\%$ of the total germicidal efficiency of the plasma jet on *E. coli*. We believe that the rest of the germicidal efficiency ($13.3 \pm 3.2\%$) can be attributed to the oxidative species formed by the jet (O , H_2O_2 , O_3 , OH , $\text{HO}_2\text{...}$) and the possible synergy between the different germicidal sources of the jet. Experiments are currently carried out to confirm this last point.

REFERENCES

- [1] G. Wattieaux, M. Yousfi, and N. Merbahi. Optical emission spectroscopy for quantification of ultraviolet radiations and biocide active species in microwave argon plasma jet at atmospheric pressure. *Spectrochimica Acta Part B: Atomic Spectroscopy*, 89(0):66 – 76, 2013.
- [2] O Motret, C Hibert, S Pellerin, and J M Povesle. Rotational temperature measurements in atmospheric pulsed dielectric barrier discharge - gas temperature and molecular fraction effects. *Journal of Physics D: Applied Physics*, 33(12):1493, 2000.
- [3] Tianhong Dai, Mark S Vrahas, Clinton K Murray, and Michael R Hamblin. Ultraviolet c irradiation: an alternative antimicrobial approach to localized infections? *Expert Rev Anti Infect Ther.*, 10(2):185–195, 2012.
- [4] Inc. Malcolm Pirnie *et al.* Ultraviolet disinfection guidance manual for the final long term 2 enhanced surface water treatment rule. Technical report, U.S. Environmental Protection Agency, Office of Water (4601), 2006.